Identification of Coagulation Factor VIII A2 Domain Residues Forming the Binding Epitope for Low-Density Lipoprotein Receptor-Related Protein[†,‡]

Andrey G. Sarafanov,[*,§] Evgeny M. Makogonenko,[§] Igor V. Pechik,[||] Klaus-Peter Radtke,[⊥] Alexey V. Khrenov,[§] Natalya M. Ananyeva,[§] Dudley K. Strickland,[@] and Evgueni L. Saenko[§]

Department of Biochemistry and Molecular Biology, University of Maryland School of Medicine, Baltimore, Maryland 21201, Center for Advanced Research in Biotechnology, University of Maryland Biotechnology Institute and National Institute of Standards and Technology, Rockville, Maryland 20850, Biolex, Inc., Pittsboro, North Carolina 27312, and Department of Surgery and Physiology, University of Maryland School of Medicine, Baltimore, Maryland 21201

Received October 7, 2005; Revised Manuscript Received December 16, 2005

ABSTRACT: Regulation of the coagulation factor VIII (fVIII) level in circulation involves a hepatic receptor low-density lipoprotein receptor-related protein (LRP). One of two major LRP binding sites in fVIII is located within the A2 domain (A2), likely exposed within the fVIII complex with von Willebrand factor and contributing to regulation of fVIII via LRP. This work aimed to identify A2 residues forming its LRP-binding site, previously shown to involve residues 484−509. Isolated A2 was subjected to alanine-scanning mutagenesis followed by expression of a set of mutants in a baculovirus system. In competition and surface plasmon resonance assays, affinities of A2 mutants K466A, R471A, R484A, S488A, R489A, R490A, H497A, and K499A for LRP were found to be decreased by 2−4-fold. This correlated with 1.3−1.5-fold decreases in the degree of LRP-mediated internalization of the mutants in cell culture. Combining these mutations into pairs led to cumulative effects, i.e., 7−13-fold decrease in affinity for LRP and 1.6−2.2-fold decrease in the degree of LRP-mediated internalization in cell culture. We conclude that the residues mentioned above play a key role in formation of the A2 binding epitope for LRP. Experiments in mice revealed an ∼4.5 times shorter half-life for A2 in the circulation in comparison with that of fVIII. The half-lives of A2 mutant R471A/R484A or A2 co-injected with receptor-associated protein, a classical ligand of LRP, were prolonged by ∼1.9 and ∼3.5 times, respectively, compared to that of A2. This further confirms the importance of the mutated residues for interaction of A2 with LRP and suggests the existence of an LRP-dependent mechanism for removing A2 as a product of dissociation of activated fVIII from the circulation.

fVIII[1] plays an essential role in blood clotting, and its functional deficiency leads to a coagulation disorder, hemophilia A, which is treated by infusions of fVIII (*1*). In the intrinsic pathway of coagulation, fVIII functions as a cofactor for fIXa to activate fX, which participates in further reactions of blood coagulation (*2*). fVIII is synthesized in liver cells as a large polypeptide (∼300 kDa) composed of the A- and C-type domains and the B domain, which are arranged in an A1−A2−B−A3−C1−C2 order (*3*). fVIII is secreted as a heterodimer consisting of A1−A2−B (heavy chain, 90−220 kDa with a variable-length B domain) and A3−C1−C2 (light chain, 80 kDa) portions linked via a Me^{2+} bond (*4*). In blood, fVIII circulates in complex with von Willebrand factor (*5*) and at the sites of coagulation is activated by thrombin or fXa into an A1/A2/A3−C1−C2 heterotrimer. This leads to dissociation of vWf and participation of fVIIIa in coagulation reactions (*6*, *7*).

Regulation of the fVIII level is mediated by LRP, a multifunctional receptor with broad ligand specificity predominantly expressed on hepatic cells (*8*). In blood, LRP is involved in clearance of lipoproteins, lipases, proteinases and

[†] This research was supported by NIH Grants HL 66101 and HL 72929 and a Judith Graham Postdoctoral Research Fellowship from National Hemophilia Foundation.

[‡] The nucleotide sequences for the pFastBac1-HM vector and fVIII and LRP genes are deposited in GenBank as accession numbers AY598466, X01179, and X13916, respectively. The amino acid sequence of fVIII can be accessed through NCBI Protein Database as entry P00451; the atomic coordinates of the model of fVIII are available from the HAMSTeRS database (http://europium.csc.mrc.ac.uk).

* To whom correspondence should be addressed. Telephone: (410) 706-8227. Fax: (410) 706-8121. E-mail: asarafanov@som.umaryland.edu.

[§] Department of Biochemistry and Molecular Biology, University of Maryland.

[||] Center for Advanced Research in Biotechnology, University of Maryland.

[⊥] Biolex, Inc.

[@] Department of Surgery and Physiology, University of Maryland.

[1] Abbreviations: fV, fVII, fVIII, fIX, and fX and fVa, fVIIa, fVIIIa, fIXa, and fXa, coagulation factors V, VII, VIII, IX, and X and their activated forms, respectively; HCh, heavy chain of fVIII; LCh, light chain of fVIII; A2, A2 domain of fVIII(a); A1/A3−C1−C2, heterodimer of fVIIIa; vWf, von Willebrand factor; LRP, low-density lipoprotein receptor-related protein; LDLR, low-density lipoprotein receptor; VLDLR, very low-density lipoprotein receptor; CR, complement-type repeats; RAP, receptor-associated protein; pd-A2, isolated plasma-derived A2 domain of fVIIIa; r-A2 or wt-A2, recombinant A2 domain of fVIIIa; hx-A2, six-His-tagged r-A2; PS, phosphatidylserine; PC, phosphatidylcholine; SD, standard deviation; HBS, 20 mM HEPES (pH 7.4)/0.15 M NaCl/0.005% Tween 20 buffer; HBS-Ca, HBS containing 2 mM $CaCl_2$; MEF, mouse embryonic fibroblast cells; SPR, surface plasmon resonance.

10.1021/bi0520380 CCC: $33.50
Published on Web 01/24/2006

proteinase−inhibitor complexes (*9*), and, in particular, some coagulation factors (*10*−*13*). LRP belongs to the LDLR family, a large group of endocytic receptors which have similar structure but different patterns of tissue expression (*14*). The ligand-binding sites of these receptors are formed by homologous CRs grouped in clusters (*15*, *16*). LRP has four clusters, with clusters II and IV being responsible for the binding of a majority of ligands (*17*). In most cases, these interactions are antagonized by RAP, a folding chaperone for LDLR family receptors which serves as a useful tool in studying such interactions (*18*, *19*).

The conclusion of involvement of LRP in clearance of fVIII from the circulation is based on several lines of experimental evidence. In clearance experiments in mice, the half-life of fVIII in the circulation could be prolonged by 3-fold by co-injection of RAP (*20*−*22*). Consistent with this finding, adenovirus-mediated overexpression of RAP in normal mice resulted in a 3.5-fold increase in the plasma fVIII level (*23*). Inactivation of the LRP gene in conditional LRP-deficient mice also led to a 2-fold prolongation of the fVIII half-life and an increase in plasma fVIII level compared to that in normal mice (*23*, *24*). Recently, it has been reported that LRP acts in concert with another member of the LDLR family, LDL receptor, in clearance of fVIII. This was demonstrated by a more significant, ∼5-fold, prolongation of the fVIII lifetime in mice with the LDLR/LRP double deficiency (*24*).

Structural studies demonstrated that fVIII has two high-affinity binding sites for LRP, located within the A2 domain (region of residues 484−509) and the A3 domain (region of residues 1811−1818), and a low-affinity binding site within the C2 domain (*20*, *25*, *26*). In vitro experiments suggest that the A3 and C2 sites are likely to be blocked by vWf bound to LCh within the circulating fVIII−vWf complex (*26*−*28*) that is consistent with a shorter half-life of fVIII observed in patients with severe von Willebrand disease (*29*) and in vWf-deficient mice (*22*). In contrast, the ability of an antibody recognizing the A2 region of residues 484−509 to bind fVIII in the fVIII−vWf complex suggests that the A2 LRP-binding site is likely to be exposed and to contribute to regulation of the fVIII level via LRP (*20*, *30*).

Activation of fVIII leads to an increase in the affinity of the A2 site for LRP, while no additional determinants of isolated A2, distant from residues 484−509, are involved in this interaction (*31*). Within fVIIIa, A2 is bound weakly to the A1/A3−C1−C2 heterodimer, and dissociation of these fragments represents a primary mechanism of spontaneous inactivation of fVIIIa (*32*−*34*).

The aim of this study was to identify amino acid residues which constitute the binding epitope of the fVIII A2 domain for LRP. To eliminate the contribution of other LRP-binding sites of fVIII, we performed our studies using isolated A2. On the basis of the 3D model of fVIII (*35*), we subjected the region of residues 484−509 and residues located nearby on the surface of A2 to alanine-scanning mutagenesis. A set of mutants was expressed in insect cells and tested for interactions with LRP under different conditions. Using this approach, we identified the residues most critical for the binding to LRP and generated a model of the LRP-binding site within the A2 domain of fVIII.

EXPERIMENTAL PROCEDURES

Proteins and Reagents. fVIII was purified from concentrated antihemophilic factor (human) (Baxter/Hyland Healthcare Inc., Glendale, CA) as described previously (*36*). fVIII HCh and LCh were prepared as described previously (*28*). A2 and the A1/A3−C1−C2 heterodimer were prepared from thrombin-activated fVIII as described previously (*6*, *37*) and purified by affinity chromatography using Sepharose with immobilized anti-A2 mAb 8860 and anti-C2 domain mAb NMC-VIII/5 (D. Scandella, American Red Cross, Rockville, MD), respectively (*38*). LRP was isolated from human placenta as described previously (*39*). RAP was expressed and purified as described previously (*40*). Anti-A2 mAbT5 was a gift from C. Fulcher (Scripps Clinic and Research Foundation, La Jolla, CA). mAbR8B12 was purchased from Green Mountain Antibodies (Burlington, VT). mAb8860 was provided by Baxter/Hyland Healthcare Inc., and mAb413 was prepared as described previously (*41*). fX, fXa, and fIXa were purchased from Enzyme Research Laboratories Inc. (South Bend, IN). Phospholipid vesicles containing 25% PS and 75% PC were prepared as described previously (*42*).

Preparation of Plasmid Constructs. fVIII cDNA cloned in the pMT2/fVIII plasmid was obtained from S. Pipe (University of Michigan, Ann Arbor, MI). The A2 coding region was amplified by PCR using the pMT2/fVIII plasmid as a template and primers 5′-AACGAAGTCCGGAGCCAAGAAGCATCCTAAAACTTGGGTAC and 5′-ACGCATCAAGCTTCTATCTTGGTTCAATGGCATTGTTTTTACTCAGC. Using the BspEI and HindIII cleavage sites, this fragment was inserted into the pBSKSII(+)/mhgx plasmid (*43*). The obtained cassette encoded a mhgx-A2 polypeptide, which carried a secretion signal (m), a six-His tag (h), a fXa cleavage site (x), green fluorescent protein (g), and the A2 portion. Since the presence of the GFP-coding region was found to inhibit A2 secretion, it was removed using NcoI and BspEI sites and replaced with a fragment obtained by annealing oligonucleotides 5′-CATGGGCGCCTCCATCGAGGGTCGGT and 5′-CCGGACCGACCCTCGATGGAGGCGCC generating the mhx-A2 cassette. Using EcoRI and XhoI sites, it was subcloned into the pFastBac1 vector (Invitrogen, Carlsbad, CA) and sequenced using the technology of Applied Biosystems (Foster City, CA).

Site-Directed Mutagenesis of A2. Mutagenesis of the A2 domain was performed using a Quick-Change site-directed mutagenesis kit (Stratagene, La Jolla, CA), the pFastBac1/mhx-A2 plasmid as a template, and a pair of primers introducing a specific mutation. For converting selected residues into alanine, we used predominantly codon GCC, except for residues H378, K380, R471, L491, K493 (GCT codon), and K512 (GCA codon). All constructs were sequenced through the mhx-A2 cassettes.

Expression and Purification of r-A2 and Its Mutants. The stocks of recombinant baculoviruses with A2 forms were obtained on the basis of Bac-to-Bac technology (Invitrogen). Insect Sf9 cells were maintained in HyQ SFX-Insect Medium (HyClone, South Logan, UT). Upon transfection with recombinant bacmids, the cells were further incubated in the presence of 10% FBS for 4 days to ensure a high level of accumulation of virus (10^9−10^{11} pfu/mL) in all viral stocks. This optimal incubation time was selected in a control experiment, when a majority of cells transfected with mhgx-

A2 cassette developed green fluorescence. Optimization of expression of A2 forms was performed using comparative titering of viral stocks for expression efficiency, developed by us previously (*44*). Typically, for expression, we used 1−20 μL of a viral stock to infect 120 mL of 1.5×10^6 cells/mL followed by incubation of the cultures for 3 days.

The secreted A2 forms were purified by affinity chromatography on a column with CNBr-activated Sepharose 4B with immobilized mAb8860. Once the medium was passed, the column was washed with HBS-Ca and 1 M NaCl. Bound proteins were eluted with HBS-Ca and 50% ethylene glycol and passed through a PD-10 column (Amersham Biosciences Corp., Piscataway, NJ), and the proteins were concentrated using an Amicon Ultra 4 centrifugal filter (Millipore, Bedford, MA). To remove the poly-His tag portions, the proteins were treated with 1% (w/w) fXa for 2 h at 25 °C, followed by removal of fXa by Xarrest agarose (Novagen, Madison, WI) and dialysis versus HBS-Ca. The average yield was 200 μg of r-A2 per 100 mL of medium. Expression levels and homogeneity of purified proteins were assessed by SDS−PAGE (10 or 4−12% gradient gels, under reducing or nonreducing conditions, Coomassie staining) and Western blot analysis using India-His-Probe reagent (Pierce, New York, NY) or mAbR8B12 for detection. The purified proteins were kept at −80 °C.

Expression and Purification of LRP Clusters II−IV. The coding regions of LRP clusters encompassing complement-type repeats 3−10 (cluster II, residues 831−1165), 11−20 (cluster III, residues 2501−2924), and 21−31 (cluster IV, residues 3312−3765) were generated by PCR using pSecTag vector-based constructs bearing these regions of LRP cDNA (obtained from I. Mikhailenko, University of Maryland, Baltimore, MD) and corresponding oligonucleotides. The fragments were further cloned into pFastBac1-HM vector using restriction endonuclease NcoI and XhoI sites. The obtained constructs were used for generation of recombinant baculoviruses, from which LRP clusters II−IV were expressed in a manner similar to that of r-A2 and purified as follows. The collected medium containing a secreted LRP fragment was dialyzed into HBS-Ca buffer with a 12−14 kDa molecular mass cutoff membrane and passed through 3 mL of poly-His tag affinity resin Talon Superflow (BD Biosciences, Palo Alto, CA). The column was washed with HBS-Ca, 1 M NaCl, and 5 mM imidazole, followed by elution of the LRP fragment with HBS-Ca, 0.3 M NaCl, and 150 mM imidazole. The eluted protein was dialyzed into HBS-Ca and 0.3 M NaCl, and its monomer form was further isolated by size-exclusion chromatography using a Superdex-200 column (Amersham Biosciences). The obtained proteins were concentrated using Amicon Ultra-4 10 kDa molecular mass cutoff membranes (Millipore Corp., Billerica, MA) and quantitated spectrophotometrically using absorbance coefficients determined on the basis of the analysis of amino acid composition with ExPASy server facilities (http://us.expasy.org/tools/protparam.html). The purified proteins were tested by PAGE (nonreducing conditions, Coomassie staining) for homogeneity and kept frozen at −80 °C.

fVIIIa Reconstitution Assay. A1/A3−C1−C2 (20 nM) and pd-A2, r-A2, or A2 (10 nM) mutant were incubated in 25 mM histidine (pH 6.0) containing 0.01% Tween 20, 0.05 M NaCl, and 100 μg/mL BSA for 30 min. The resulting fVIIIa activity was determined either in a purified system with fXa chromogenic substrate S-2765 (Chromogenix, Mölndal, Sweden) (*45*, *46*) or in a one-stage clotting assay with human fVIII-deficient plasma (George King Bio-Medical, Inc., Overland Park, KS) using fVIII standard MEGA1 (Food and Drug Administration, Bethesda, MD) (*47*).

SPR-Based Assay for Studying the Binding of r-A2 Forms to LRP, Its Clusters II−IV, and A1/A3−C1−C2. The measurements were performed using a Biacore 3000 instrument (Biacore, Uppsala, Sweden). LRP, its clusters II−IV, or A1/A3−C1−C2 was covalently immobilized on a CM5 chip using an amine coupling kit (Biacore) and tested in the binding experiments as described in refs *17* and *48* and ref *49*, respectively. The immobilization levels were ∼7 fM/mm^2 for LRP, ∼15 fM/mm^2 for each LRP cluster, and ∼40 fM/mm^2 for A1/A3−C1−C2. Association of the A2 forms with immobilized LRP or its clusters and with immobilized A1/A3−C1−C2 was tested in HBS-Ca and in 25 mM histidine (pH 6.0), 0.05 M NaCl, 2 mM $CaCl_2$, and 0.005% Tween 20, respectively, at a flow rate of 15 μL/min. The dissociation of bound proteins was recorded by replacing the ligand-containing buffer with buffer alone. The level of nonspecific binding corresponding to the ligand binding to the uncoated chip was subtracted from the signal. Chips were regenerated by washing with 0.1 M H_3PO_4 for immobilized LRP and its clusters, and with 25 mM Tris (pH 8.0), 1 M NaCl, 0.35 M $CaCl_2$, and 0.005% Tween 20 for immobilized A1/A3−C1−C2. The kinetic parameters were derived from the binding and dissociation curves using Biacore software BIAevaluation version 3.2. The binding of A2 forms to LRP was fitted to a heterogeneous ligand (two-site) model, and the binding to LRP clusters and to A1/A3−C1−C2 was fitted to a 1:1 (Langmuir) model.

Radiolabeling of r-A2, Its Mutants, and fVIII. Labeling was performed in a manner similar to that described for fVIII (*30*). Proteins were dialyzed into 0.2 M sodium acetate (pH 6.8) and 5 mM calcium nitrate. Ten micrograms of each protein in 50 μL was mixed with 5 μL of lactoperoxidase beads (Worthington Biochemical Corp., Freehold, NJ) and 5 μL of Na^{125}I solution (100 mCi/mL, Amersham Biosciences). The reaction was started by adding 5 μL of 0.03% H_2O_2 and proceeded for 4 min at 20 °C. Unreacted Na^{125}I was removed by size-exclusion chromatography. The specific radioactivity was $\sim 5 \times 10^6$ cpm/μg of protein.

Cell-Mediated Surface Binding and Internalization of r-A2 and Its Mutants. LRP-expressing MEF cells and LRP-deficient PEA 13 cells were obtained from J. Herz (University of Texas Southwestern Medical Center, Dallas, TX) and maintained in DMEM and 10% FBS as described previously (*50*). For the experiment, the cells were seeded at a density of $\sim 1.5 \times 10^5$ cells/well in 12-well plates and incubated overnight to ∼80% confluence. This was followed by incubation of the cells with ^{125}I-labeled r-A2 or its mutants (0−80 nM) in 0.5 mL of medium containing 1% BSA in the absence or presence of RAP (1 μM) for 4 h. The surface binding and internalization of radiolabeled proteins were assessed as described previously (*51*, *52*). Briefly, after being incubated, cells were washed with HBS-Ca and treated with trypsin to release the cell surface-bound radioactivity. The radioactivity, which remained associated with the cells, was considered internalized.

Clearance of A2 Forms from the Circulation in Mice. Prior to experiments, the proteins were labeled with ^{125}I as

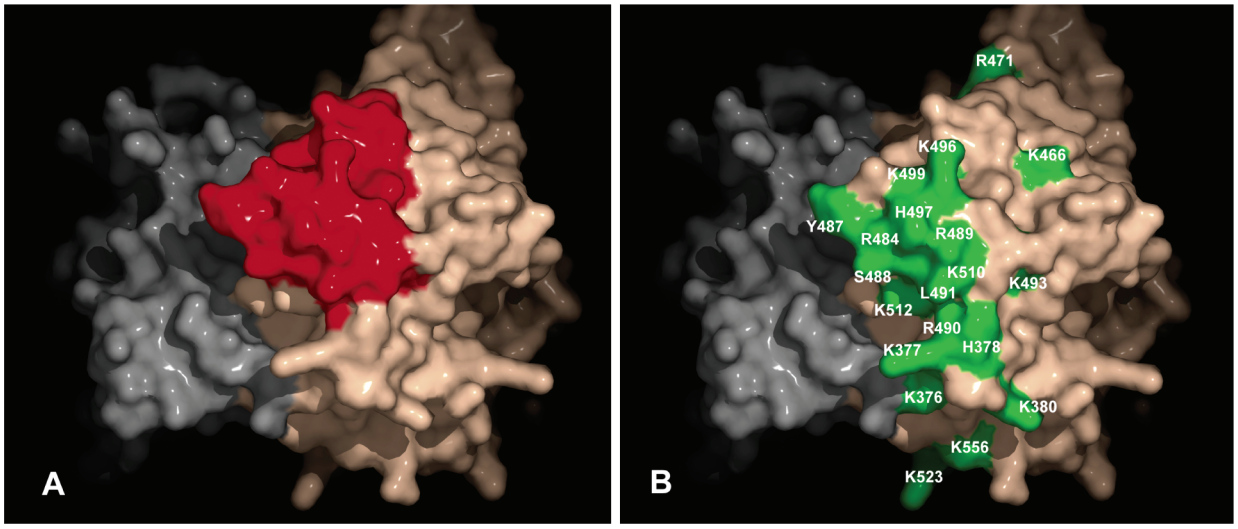

FIGURE 1: Alanine-scanning mutagenesis of the fVIII A2 domain. Fragment of the atomic model of membrane-bound fVIII (B domain deleted) represented by the solvent-accessible surface featuring the A1 (gray) and A2 (beige) domains. The A2 region of residues 484−509 involved in binding to LRP is colored red (A), and the residues subjected to mutagenesis are colored green (B). This figure was generated using the atomic model of membrane-bound fVIII and PyMOL (http://www.pymol.org).

described above. Either [^{125}I]A2 (100 nM) (alone or in the presence of 200 μM RAP), the [^{125}I]A2 R471A/R484A (100 nM) or [^{125}I]A2 K380A/K523A (100 nM) double-point mutant, or [^{125}I]fVIII (100 nM) in 100 μL of HBS-Ca was injected into the tail vein of BALB/c mice (12−14 weeks old, weight of ∼25 g), with four mice in each group. Clearance of the radiolabeled proteins from the circulation was monitored as previously described (*20*, *30*). Briefly, blood samples were withdrawn from each mouse via retro-orbital puncture at time intervals within a 1−180 min range, and the radioactivity of the samples was measured using a gamma-counter. The values were normalized to the sample volumes, expressed as a percentage of the initial count (sample taken at 1 min), and the data were fitted using a double-exponential decay model with SigmaPlot version 8.0 (SYSTAT Software, Point Richmond, CA) as described previously (*20*, *23*).

RESULTS

Expression and Characterization of A2 and Its Mutants. To generate A2 mutants, we used a baculovirus expression system which provides the folding and post-translational modification of proteins in a manner similar to that of mammalian cells. In the scanning mutagenesis of the region of residues 484−509 (Figure 1A) and its vicinity, we predominantly targeted positively charged residues mostly responsible for the binding of ligands to members of the LDLR family, and also residues with hydrophobic and hydroxyl groups shown to contribute to the binding (*53*−*55*). The selected residues (Figure 1B) were converted into alanines, generating a panel of 20 single-point A2 mutants. The secretion levels of the mutants were similar to that of nonmutated r-A2 (wt-A2), except for the mutants K466A and R471A which secreted less efficiently (Figure 2A,B). As demonstrated by PAGE and Western blot analysis, all A2 mutants were isolated from culture media with a purity similar to that shown for wt-A2 in Figure 2C. To assess the effect of mutations on A2 conformation, we compared fluorescence spectra of the mutants and those of recombinant A2 (wt-A2) and plasma-derived A2 (pd-A2). The spectral maxima of all A2 mutants were found to be identical to those of intact wt-A2 and pd-A2, whereas the maximum of denaturated wt-A2 was shifted from 336 to 350 nm in comparison with the native form in a control experiment (data not shown). This indicates that the mutations did not affect the conformation of A2.

The equivalency of wt-A2 to pd-A2 was tested in two assays. First, we compared the effect of mAb413 on interaction of both forms of A2 and LRP in a solid-phase binding assay as we previously described for fVIII and LRP (*20*). This antibody, which recognizes the region of residues 484−509 in the A2 domain (*56*), inhibited the interaction of fVIII with LRP (K_i ∼ 2.5 nM), which was the initial observation for mapping the LRP-binding site within A2. We found that mAb413 also inhibited the binding of pd-A2 and r-A2 to immobilized LRP in a dose-dependent manner with K_i values of ∼1.3 and ∼1.8 nM, respectively (Figure 3A). The similarity of these values reflects the similar organization of the binding sites for mAb413 and, consequently, for LRP in wt-A2 and pd-A2. No inhibition of the binding of pd-A2 and r-A2 to LRP was observed by mAbs R8B12 and T5, which have epitopes within the C-terminal part of A2 (*57*, *58*).

Next, we tested the ability of recombinant A2 (wt-A2) to reconstitute fVIIIa and to support its cofactor function, which requires the involvement of multiple regions of A2 (*59*−*62*). We found that r-A2 was able to associate with A1/A3−C1−C2 and form functionally active fVIIIa as detected in a coagulation assay (*47*). While the clotting activity of chimeric fVIIIa was lower than that of fVIIIa reconstituted with pd-A2 (Figure 3B), it was similar to the reported activity of fVIIIa reconstituted with recombinant A2 expressed in CHO cells (*63*). Thus, though the activity test showed a slight difference between pd-A2 and r-A2, the binding and spectroscopy tests demonstrated their similarity, in particular in the arrangement of the LRP-binding site, and substantiated the consequent mutagenic analysis of A2.

Interaction of A2 Mutants and LRP in a Solid-Phase Competition Assay. To identify A2 residues that are important for interaction with LRP, we compared effects of increasing

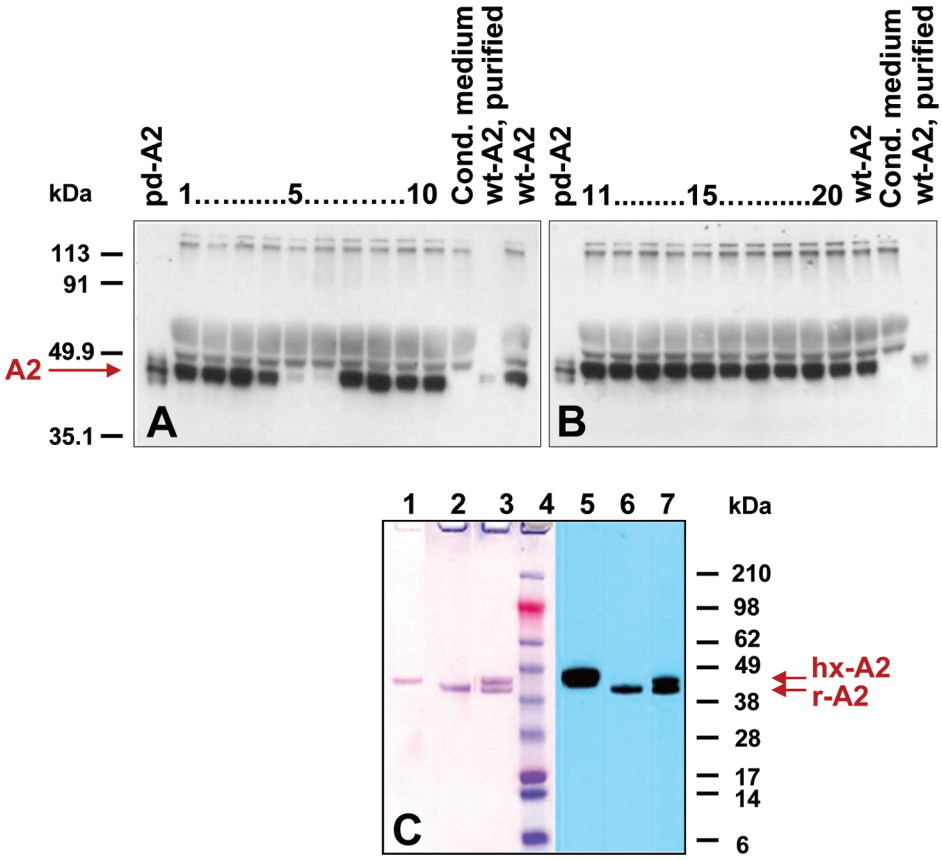

FIGURE 2: Expression and purification of A2 mutants. (A and B) Secretion of A2 forms in culture medium. The aliquots were resolved by PAGE (10% gel, reducing conditions) followed by transfer of proteins on a membrane and detection of A2 forms with anti-A2 mAbR8B12. The sample numbering for A2 mutants corresponds to that shown in Table 1. Samples of purified wt-A2, pd-A2, and conditioned medium taken from cells not infected by baculovirus (controls) are also shown. (C) Example of protein purification shown for wt-A2: lanes 1−4, PAGE analysis (4−12% gel, nonreducing conditions); and lanes 5−7, Western blot analysis performed as described above. Lanes 3 and 7 show two forms of wt-A2 (hx-A2, poly-His-tagged, and r-A2, nontagged forms) presented in the culture medium. Lanes 1 and 5 show hx-A2 isolated on anti-poly-His tag affinity sorbent and lanes 2 and 6 purified wt-A2 after removal of the His tag. Lane 4 contain molecular mass markers.

concentrations of each A2 mutant and wt-A2 on the binding of [^{125}I]pd-A2 to LRP immobilized in 96-well plates as previously described for the interaction of fVIII with LRP (*20*). We found that while the inhibitory effect of most of the mutants was very close to that of recombinant wt-A2 (K_i = 29−38 nM), eight mutants, K466A, R471A, R484A, S488A, R489A, R490A, H497A, and K499A, were less effective as competitors as shown for representative mutants in Figure 4A. The corresponding K_i values were ∼2−5-fold higher compared with that of wt-A2 (Table 1), indicating the importance of these positions for the interaction with LRP.

Interaction of A2 Mutants and LRP in a SPR-Based Assay. To gain deeper insight into the mechanism of interaction of A2 and LRP, we first studied the real-time binding of pd-A2 to LRP immobilized on a sensor chip. Figure 5A shows a representative signal corresponding to association and dissociation of pd-A2 (250 nM) and immobilized LRP. The families of binding curves obtained for five different concentrations of A2 (10−250 nM) were fitted to a two-site binding model. This model was used on the basis of the ability of thrombin-cleaved HCh of fVIII [i.e., A2 (*20*)] to interact with clusters II and IV of LRP (*31*) and was also previously used to fit the binding of fVIII LCh to LRP (*25*). The resulting kinetic constants determined on the basis of the association and/or dissociation rate indicated the presence

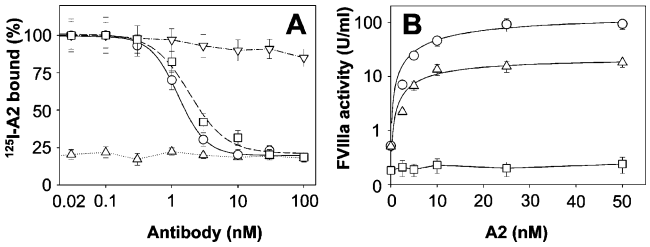

FIGURE 3: Comparison of properties of plasma-derived and recombinant A2. (A) Effects of anti-A2 monoclonal antibodies on the binding of pd-A2 and r-A2 to immobilized LRP. One nanomole of ^{125}I-labeled pd-A2 (○) or r-A2 (□) was incubated in LRP-coated wells of 96-well plates in HBS-Ca in the presence of mAb413 used at the indicated concentrations. In control experiments, [^{125}I]pd-A2 was incubated in the presence of mAbR8B12 (▽, dashed−dotted line) and in BSA-coated wells (△, dotted line). The amount of bound radioactivity is expressed as a percentage of the corresponding signal in the absence of the corresponding antibody. Each point represents the mean of triplicate determinations with the SD. The fits of the data for pd-A2 (solid) and r-A2 (dashed) to a heterologous displacement model using SigmaPlot version 8.0 are shown. (B) Activity of reconstituted fVIIIa using pd-A2 or r-A2. pd-A2 (○) or r-A2 (△) was incubated at the indicated concentrations with 20 nM A1/A3−C1−C2 in 25 mM histidine (pH 6.0), 0.05 M NaCl, 0.01% Tween 20, and 100 μg/mL BSA buffer for 30 min. In the control experiment, pd-A2 was incubated in the absence of A1/A3−C1−C2 (□). The resulting fVIIIa activity was measured in a one-stage clotting assay. Each data point represents the mean of duplicate measurements and the SD.

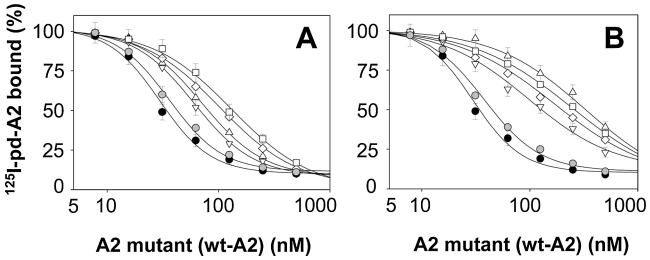

FIGURE 4: Binding of pd-A2 to LRP in the presence of selected A2 mutants in a solid-phase assay. [^{125}I]pd-A2 (2 nM) was incubated in LRP-coated wells of 96-well plates in HBS-Ca buffer in the presence of A2 mutants used at the indicated concentrations for 2 h at 37 °C: (A) r-A2 (wt-A2) (●) and A2 single-point mutants L491A (gray circles), K466A (□), R484A (△), S488A (▽), and R489A (◇) and (B) r-A2 (wt-A2) (●) and A2 double-point mutants K380A/K512A (gray circles), K466A/R489A (□), R471A/R484A (△), S488A/K499A (▽), and R490A/H497A (◇). After incubation, the wells were counted for bound radioactivity. The values were corrected for nonspecific binding (<10%) determined by binding of [^{125}I]A2 to BSA-coated wells and expressed as a percentage of the bound [^{125}I]A2 in the absence of a competitor. Each point represents the mean of duplicate experiments and the SD. The lines show best fits of the data to a heterologous displacement model (SigmaPlot version 8.0).

of higher-affinity (class 1) and lower-affinity (class 2) A2 binding sites in LRP: $K_D(1) = 14 \pm 2$ nM [$k_{on} = (6.2 \pm 0.6) \times 10^4$ M^{-1} s^{-1}, $k_{off} = (8.7 \pm 0.9) \times 10^{-4}$ s^{-1}] and $K_D(2) = 29 \pm 5$ nM [$k_{on} = (3.1 \pm 0.4) \times 10^5$ M^{-1} s^{-1}, $k_{off} = (9.0 \pm 1.1) \times 10^{-3}$ s^{-1}]. To test the relevance of the model, we similarly tested the binding of pd-A2 to immobilized isolated LRP clusters II−IV expressed in the baculovirus system. The kinetic constants were calculated using a one-site binding model. While no binding was observed for cluster III, pd-A2 was found to bind to cluster II with a K_D of 19 ± 3 nM [$k_{on} = (4.8 \pm 0.5) \times 10^4$ M^{-1} s^{-1}, $k_{off} = (9.1 \pm 1.0) \times 10^{-4}$ s^{-1}] and to cluster IV with a K_D of 36 ± 6 nM [$k_{on} = (1.8 \pm 0.2) \times 10^5$ M^{-1} s^{-1}, $k_{off} = (6.5 \pm 0.7) \times 10^{-3}$ s^{-1}] (panels B and C of Figure 5, respectively). These values correlate with kinetic constants obtained for full-length LRP, supporting the relevance of the two-site binding model. In addition, the apparent affinity of pd-A2 for LRP ($K_D = 11.7 \pm 3.5$ nM) assessed on the basis of the dependence of the equilibrium signal on A2 concentration (steady-state model) was found to be similar to the previously reported affinity of pd-A2 for LRP ($K_D = 15$ nM) determined by SPR (*31*).

Next, we similarly compared the binding of each A2 mutant and wt-A2 to immobilized LRP. The obtained pairs of K_D values (Table 1) reflected the presence of higher-affinity (class 1) and lower-affinity (class 2) binding sites in LRP, which likely correspond to clusters II and IV, respectively. To confirm this assumption, we tested the binding of wt-A2 and its mutant R471A (which showed the greatest reduction in the affinity for LRP) to immobilized clusters II and IV. The representative signals are shown in Figure 5D−F. The recorded families of binding curves were fitted to a one-site model. For cluster II, the K_D values obtained for wt-A2 and the mutant R471A were 20 ± 3 nM [$k_{on} = (3.6 \pm 0.4) \times 10^4$ M^{-1} s^{-1}, $k_{off} = (7.2 \pm 0.6) \times 10^{-4}$ s^{-1}] and 78 ± 11 nM [$k_{on} = (2.9 \pm 0.3) \times 10^4$ M^{-1} s^{-1}, $k_{off} = (2.3 \pm 0.2) \times 10^{-3}$ s^{-1}], respectively. For cluster IV, the K_D values for wt-A2 and the mutant R471 were 39 ± 8 nM [$k_{on} = (2.4 \pm 0.3) \times 10^5$ M^{-1} s^{-1}, $k_{off} = (9.4 \pm 1.4) \times 10^{-3}$ s^{-1}] and 147 ± 28 nM [$k_{on} = (1.5 \pm 0.2) \times 10^5$ M^{-1} s^{-1}, $k_{off} = (2.2 \pm 0.3) \times 10^{-2}$ s^{-1}], respectively. These results support the assumption that the parameters corresponding to the binding of A2 mutants to class 1 and 2 binding sites in LRP reflect their interactions with clusters II and IV, respectively. For a number of A2 mutants, both K_D values were increased to a similar degree, reflecting a general decrease in the mutants' affinity for LRP. The greatest increase in the K_D values (2−4-fold) was found for the same A2 mutants, K466A, R471A, R484A, S488A, R489A, R490A, H497A, and K499A, which had the highest K_i values in the competition assay (Table 1). Noteworthy is the fact that the reduction of the mutants' affinities for LRP, assessed in the competition and binding assays, was statistically significant as the corresponding K_i and K_D values were well reproduced and the increase in both values correlated.

Interactions of A2 Double-Point Mutants with LRP in a Purified System. To further verify the role of the eight identified residues of A2 for its binding to LRP, we combined their mutations in pairs to test whether this would produce more profound effects. The generated mutants of A2 were K466A/R489A, R471A/R484A, S484A/R499A, and R490A/H497A. We also prepared an additional mutant K380A/K523A, on which parental single-point substitutions had no effect for the binding to LRP, to serve as a control. In the competition experiment, all four mutants were significantly less effective as inhibitors of binding of [^{125}I]pd-A2 to immobilized LRP ($K_i \sim 124-348$ nM) than wt-A2 or A2 K380A/K523A ($K_i \sim 30$ and ~35 nM, respectively) as shown in Figure 4B and Table 1.

Consistent with these data, in the SPR-based assay, the determined K_D values for the binding of double-point mutants to immobilized LRP were increased by ~7−13-fold in comparison with that of wt-A2 or the K380A/K523A mutant (Table 1). In an additional experiment, A2 mutant R471A/R484A interacted with immobilized LRP clusters II and IV (Figure 5D−F), with K_D values of 275 ± 52 nM [$k_{on} = (1.3 \pm 0.2) \times 10^4$ M^{-1} s^{-1}, $k_{off} = (3.6 \pm 0.4) \times 10^{-3}$ s^{-1}] and 408 ± 63 nM [$k_{on} = (6.1 \pm 0.6) \times 10^4$ M^{-1} s^{-1}, $k_{off} = (2.5 \pm 0.3) \times 10^{-2}$ s^{-1}], respectively, which further confirms the relevance of the fitting model used. Thus, both methods demonstrated that the combination of A2 single-point mutations, which affected the affinity of A2 for LRP, had a cumulative effect leading to a further decrease in the affinity. In summary, experiments in a purified system indicated that A2 positions K466, R471, R484, S488, R489, R490, H497, and K499 are major contributors for its binding to LRP.

Effect of Mutations in A2 on the Functional Activity of fVIII. To assess whether introduced mutations affect fVIII cofactor activity, we tested the ability of A2 mutants to interact with the purified A1/A3−C1−C2 heterodimer and to reconstitute functionally active fVIIIa. The interactions of the mutants with A1/A3−C1−C2 were assessed in a SPR-based assay. The binding of each A2 mutant and wt-A2 to immobilized A1/A3−C1−C2 was tested at pH 6.0 (Experimental Procedures), when this complex is relatively stable [$K_D \sim 7.2$ nM (*49*)] as compared to its lower stability at pH 7.4 [$K_D \sim 260$ nM (*32*)]. The kinetic constants for complex formation were derived by fitting the binding/dissociation curves to a one-site model (Table 2). For the majority of A2 mutants, the obtained K_D values were very close to those of wt-A2 (6.7 ± 1.4 nM) and pd-A2 (6.4 ± 1.5 nM), reflecting the normal formation of the complexes. The affinities of the

Table 1: Parameters of the Interaction of A2 Mutants with LRP[a]

A2 form	K_i (nM)	$k_{on}(1)$ (M^{-1} s^{-1})	$k_{off}(1)$ (s^{-1})	$K_D(1)$ (nM)	$k_{on}(2)$ (M^{-1} s^{-1})	$k_{off}(2)$ (s^{-1})	$K_D(2)$ (nM)
wt-A2	29 ± 3	$(5.4 \pm 0.6) \times 10^4$	$(8.1 \pm 0.9) \times 10^{-4}$	15 ± 2	$(2.6 \pm 0.4) \times 10^5$	$(8.8 \pm 1.1) \times 10^{-3}$	34 ± 7
K376A	31 ± 3	$(4.2 \pm 0.4) \times 10^4$	$(6.7 \pm 0.8) \times 10^{-4}$	16 ± 2	$(2.3 \pm 0.3) \times 10^5$	$(7.1 \pm 0.9) \times 10^{-3}$	31 ± 6
K377A	28 ± 3	$(5.7 \pm 0.5) \times 10^4$	$(8.6 \pm 0.8) \times 10^{-4}$	15 ± 2	$(2.4 \pm 0.3) \times 10^5$	$(8.1 \pm 0.8) \times 10^{-3}$	34 ± 5
H378A	32 ± 4	$(4.5 \pm 0.5) \times 10^4$	$(8.6 \pm 1.1) \times 10^{-4}$	19 ± 4	$(3.0 \pm 0.5) \times 10^5$	$(9.9 \pm 1.4) \times 10^{-3}$	33 ± 7
K380A	36 ± 4	$(5.8 \pm 0.7) \times 10^4$	$(9.9 \pm 1.1) \times 10^{-4}$	17 ± 3	$(2.5 \pm 0.2) \times 10^5$	$(8.7 \pm 1.7) \times 10^{-3}$	35 ± 7
K466A	$\mathbf{132 \pm 12}$	$(2.1 \pm 0.2) \times 10^4$	$(1.1 \pm 0.1) \times 10^{-3}$	$\mathbf{54 \pm 7}$	$(1.0 \pm 0.1) \times 10^5$	$(1.1 \pm 0.2) \times 10^{-2}$	$\mathbf{106 \pm 22}$
R471A	$\mathbf{136 \pm 13}$	$(3.1 \pm 0.3) \times 10^4$	$(2.0 \pm 0.2) \times 10^{-3}$	$\mathbf{65 \pm 9}$	$(1.0 \pm 0.1) \times 10^5$	$(1.2 \pm 0.2) \times 10^{-2}$	$\mathbf{121 \pm 24}$
R484A	$\mathbf{72 \pm 6}$	$(2.3 \pm 0.2) \times 10^4$	$(1.0 \pm 0.1) \times 10^{-3}$	$\mathbf{44 \pm 6}$	$(1.1 \pm 0.2) \times 10^5$	$(9.1 \pm 1.5) \times 10^{-3}$	$\mathbf{83 \pm 20}$
Y487A	38 ± 4	$(3.6 \pm 0.5) \times 10^4$	$(9.8 \pm 1.0) \times 10^{-4}$	28 ± 5	$(2.0 \pm 0.3) \times 10^5$	$(9.8 \pm 1.2) \times 10^{-3}$	49 ± 8
S488A	$\mathbf{61 \pm 7}$	$(2.6 \pm 0.3) \times 10^4$	$(1.0 \pm 0.1) \times 10^{-3}$	$\mathbf{40 \pm 6}$	$(1.8 \pm 0.2) \times 10^5$	$(1.2 \pm 0.2) \times 10^{-2}$	$\mathbf{67 \pm 13}$
R489A	$\mathbf{103 \pm 9}$	$(2.3 \pm 0.2) \times 10^4$	$(1.1 \pm 0.2) \times 10^{-3}$	$\mathbf{47 \pm 9}$	$(1.4 \pm 0.2) \times 10^5$	$(1.3 \pm 0.2) \times 10^{-2}$	$\mathbf{93 \pm 16}$
R490A	$\mathbf{74 \pm 6}$	$(2.4 \pm 0.3) \times 10^4$	$(1.0 \pm 0.1) \times 10^{-3}$	$\mathbf{42 \pm 7}$	$(1.6 \pm 0.2) \times 10^5$	$(1.0 \pm 0.1) \times 10^{-2}$	$\mathbf{63 \pm 10}$
L491A	36 ± 4	$(4.9 \pm 0.6) \times 10^4$	$(8.8 \pm 1.1) \times 10^{-4}$	18 ± 3	$(2.0 \pm 0.2) \times 10^5$	$(6.6 \pm 0.8) \times 10^{-3}$	33 ± 8
K493A	35 ± 4	$(4.8 \pm 0.5) \times 10^4$	$(9.6 \pm 1.1) \times 10^{-4}$	20 ± 3	$(2.2 \pm 0.3) \times 10^5$	$(9.0 \pm 1.4) \times 10^{-3}$	41 ± 8
K496A	31 ± 3	$(5.0 \pm 0.4) \times 10^4$	$(9.5 \pm 1.3) \times 10^{-4}$	19 ± 3	$(2.5 \pm 0.3) \times 10^5$	$(9.0 \pm 0.9) \times 10^{-3}$	36 ± 6
H497A	$\mathbf{91 \pm 8}$	$(2.7 \pm 0.3) \times 10^4$	$(1.2 \pm 0.2) \times 10^{-3}$	$\mathbf{44 \pm 9}$	$(1.3 \pm 0.2) \times 10^5$	$(1.0 \pm 0.1) \times 10^{-2}$	$\mathbf{80 \pm 15}$
K499A	$\mathbf{64 \pm 6}$	$(2.9 \pm 0.3) \times 10^4$	$(1.2 \pm 0.2) \times 10^{-3}$	$\mathbf{43 \pm 8}$	$(1.5 \pm 0.2) \times 10^5$	$(1.0 \pm 0.1) \times 10^{-2}$	$\mathbf{69 \pm 18}$
K510A	33 ± 4	$(4.3 \pm 0.5) \times 10^4$	$(8.6 \pm 1.0) \times 10^{-4}$	20 ± 3	$(2.2 \pm 0.3) \times 10^5$	$(8.4 \pm 0.9) \times 10^{-3}$	38 ± 7
K512A	27 ± 3	$(4.4 \pm 0.4) \times 10^4$	$(7.9 \pm 1.2) \times 10^{-4}$	18 ± 3	$(3.1 \pm 0.4) \times 10^5$	$(9.6 \pm 1.3) \times 10^{-3}$	31 ± 6
K523A	31 ± 3	$(4.7 \pm 0.4) \times 10^4$	$(9.7 \pm 1.1) \times 10^{-4}$	21 ± 3	$(2.3 \pm 0.4) \times 10^5$	$(9.0 \pm 1.4) \times 10^{-3}$	39 ± 9
K556A	29 ± 3	$(4.6 \pm 0.5) \times 10^4$	$(8.7 \pm 1.4) \times 10^{-4}$	19 ± 4	$(2.5 \pm 0.4) \times 10^5$	$(7.5 \pm 1.0) \times 10^{-3}$	30 ± 6
K466A/R489A	$\mathbf{264 \pm 24}$	$(9.5 \pm 0.8) \times 10^3$	$(1.7 \pm 0.2) \times 10^{-3}$	$\mathbf{179 \pm 26}$	$(8.1 \pm 0.7) \times 10^4$	$(2.4 \pm 0.3) \times 10^{-2}$	$\mathbf{291 \pm 44}$
R471A/R484A	$\mathbf{348 \pm 31}$	$(1.5 \pm 0.2) \times 10^4$	$(3.1 \pm 0.3) \times 10^{-3}$	$\mathbf{207 \pm 34}$	$(6.3 \pm 0.6) \times 10^4$	$(2.3 \pm 0.2) \times 10^{-2}$	$\mathbf{358 \pm 46}$
S488A/R499A	$\mathbf{124 \pm 8}$	$(1.3 \pm 0.1) \times 10^4$	$(1.3 \pm 0.2) \times 10^{-3}$	$\mathbf{98 \pm 17}$	$(9.1 \pm 0.7) \times 10^4$	$(1.7 \pm 0.2) \times 10^{-2}$	$\mathbf{187 \pm 26}$
R490A/H497A	$\mathbf{178 \pm 15}$	$(1.4 \pm 0.1) \times 10^4$	$(1.7 \pm 0.2) \times 10^{-3}$	$\mathbf{124 \pm 17}$	$(7.6 \pm 0.7) \times 10^4$	$(1.8 \pm 0.2) \times 10^{-2}$	$\mathbf{241 \pm 35}$
K380A/K523A	35 ± 4	$(4.5 \pm 0.4) \times 10^4$	$(9.5 \pm 0.7) \times 10^{-4}$	22 ± 3	$(2.1 \pm 0.2) \times 10^5$	$(8.4 \pm 0.8) \times 10^{-3}$	40 ± 5

[a] A2 mutants and wt-A2 were tested at different concentrations for their ability to inhibit binding of [^{125}I]pd-A2 to immobilized LRP in the assay described in Figure 4. The data were fitted to a heterologous displacement model, and the corresponding K_i values were determined. In SPR-based experiments, A2 mutants and wt-A2 were tested at different concentrations for binding to immobilized LRP as described in Experimental Procedures. The kinetic constants were derived using a two-site binding model and correspond to the presence of two classes of binding sites in LRP. A2 mutants, which had the greatest decrease in affinity for LRP, and their K_i and K_D values are shown in bold. Data represent the means and SD obtained in three measurements.

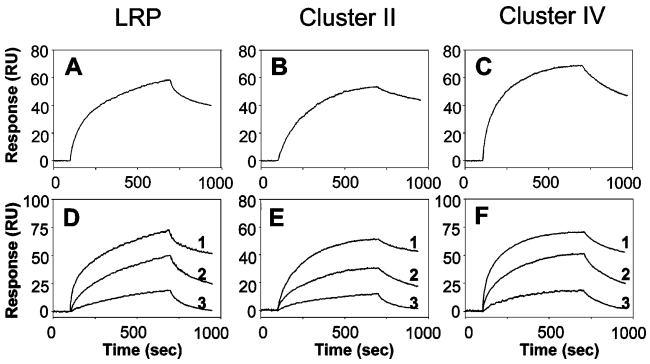

FIGURE 5: Binding of pd-A2, r-A2, and A2 mutants to LRP and its clusters II and IV in a SPR-based assay. LRP (A and D) and clusters II (B and E) and IV (C and F) were immobilized on a sensor chip at ~7 fM/mm^2 (LRP) and ~15 fM/mm^2 (clusters) and tested for binding in HBS-Ca buffer with each form of A2 at 250 nM: (A−C) pd-A2 and (D−F) r-A2 (curve 1), A2 mutant R471A (curve 2), and A2 mutant R471A/R484A (curve 3). Dissociation was recorded upon replacement of the ligand solution with the buffer. Regeneration of chips was performed by washing with 0.1 M H_3PO_4. The signals are indicated in resonance units (RU) corrected for nonspecific binding of A2 to a blank chip.

K376A−K380A mutants were slightly decreased, likely reflecting the impaired interactions with the A1 domain contact area within reconstituted fVIIIa (*59*). Generally, the introduced mutations did not affect the internal stability of fVIIIa.

The functional activity of the reconstituted fVIIIa forms was assessed in chromogenic and one-stage clotting assays. Both methods produced comparable values of the relative activities, which varied in the range of 1−100% of the activity of fVIIIa reconstituted with wt-A2 (Table 2). The decrease in the functional activity of A2 mutants K376A−K380A correlated with the slight reduction in their affinity for A1/A3−C1−C2. Notably, the majority of A2 single-point mutants with reduced affinity for LRP (the mutants R484A, S488A, R489A, R490A, and H497A) retained a cofactor activity close to normal. This further confirms that the reduction in A2 mutants' affinity for LRP was due to specific targeting of the LRP-binding epitope but not due to an effect on the general structure of the molecule. In addition, for double-point A2 mutants, introduction of the second mutation did not affect markedly the A2 internal stability and functional activity in reconstituted fVIIIa (Table 2).

LRP-Mediated Internalization of A2 Mutants in Cell Culture. We previously demonstrated that isolated A2 can be catabolized via LRP in cell culture, like fVIII (*30*). To test the role of the above eight residues of A2 in interaction with LRP natively exposed on the cell surface, we compared LRP-mediated internalization of the corresponding mutants and wt-A2 by MEF cells expressing this receptor. As additional controls, we tested the A2 mutants L491A and K380A/K523A, affinities for LRP of which were similar to that of wt-A2. While the binding of all tested forms of A2 to the cells was similar (SD = 11−14%, data not shown), their internalization varied. For the single-point mutants, it constituted 68−81% (SD = 10−13%) of wt-A2 and A2 L491A levels (Figure 6A). For the double-point mutants, the internalization levels varied within a range of 46−65% (SD = 10−14%) of wt-A2 and A2 K380A/K523A levels (Figure 6B).

The presence of RAP did not affect the surface binding of any A2 form (data not shown), consistent with our

Table 2: Parameters of the Interaction of A2 Mutants with A1/A3−C1−C2 and Relative Activities of Reconstituted fVIIIa Molecules[a]

A2 form	k_{on} (M^{-1} s^{-1})	k_{off} (s^{-1})	K_D (nM)	activity in the chromogenic assay (%)	activity in the clotting assay (%)
wt-A2	$(1.4 \pm 0.2) \times 10^5$	$(9.4 \pm 2.1) \times 10^{-4}$	7 ± 2	100 ± 8	100 ± 5
K376A	$(8.0 \pm 0.9) \times 10^4$	$(1.5 \pm 0.2) \times 10^{-3}$	19 ± 3	36 ± 4	48 ± 3
K377A	$(7.9 \pm 0.7) \times 10^4$	$(1.2 \pm 0.2) \times 10^{-3}$	15 ± 3	46 ± 4	63 ± 3
H378A	$(8.4 \pm 0.9) \times 10^4$	$(2.0 \pm 0.3) \times 10^{-3}$	14 ± 3	53 ± 5	64 ± 3
K380A	$(9.1 \pm 0.9) \times 10^4$	$(1.5 \pm 0.2) \times 10^{-3}$	16 ± 3	50 ± 4	48 ± 2
K466A	$(1.1 \pm 0.1) \times 10^5$	$(9.7 \pm 0.8) \times 10^{-4}$	9 ± 2	31 ± 4	16 ± 2
R471A	$(1.3 \pm 0.2) \times 10^5$	$(1.0 \pm 0.2) \times 10^{-3}$	8 ± 2	11 ± 3	12 ± 1
R484A	$\mathbf{(1.2 \pm 0.1) \times 10^5}$	$\mathbf{(9.7 \pm 0.8) \times 10^{-4}}$	$\mathbf{8 \pm 1}$	$\mathbf{94 \pm 7}$	$\mathbf{92 \pm 5}$
Y487A	$(1.2 \pm 0.1) \times 10^5$	$(9.0 \pm 1.0) \times 10^{-4}$	8 ± 1	39 ± 5	41 ± 3
S488A	$\mathbf{(1.6 \pm 0.2) \times 10^5}$	$\mathbf{(1.3 \pm 0.3) \times 10^{-3}}$	$\mathbf{8 \pm 2}$	$\mathbf{97 \pm 8}$	$\mathbf{106 \pm 4}$
R489A	$\mathbf{(1.7 \pm 0.3) \times 10^5}$	$\mathbf{(1.2 \pm 0.2) \times 10^{-3}}$	$\mathbf{7 \pm 2}$	$\mathbf{91 \pm 5}$	$\mathbf{89 \pm 3}$
R490A	$\mathbf{(1.5 \pm 0.2) \times 10^5}$	$\mathbf{(1.3 \pm 0.2) \times 10^{-3}}$	$\mathbf{9 \pm 2}$	$\mathbf{82 \pm 7}$	$\mathbf{75 \pm 4}$
L491A	$(1.0 \pm 0.1) \times 10^5$	$(8.1 \pm 0.7) \times 10^{-4}$	8 ± 1	101 ± 9	104 ± 7
K493A	$(2.0 \pm 0.3) \times 10^5$	$(1.6 \pm 0.2) \times 10^{-3}$	8 ± 2	82 ± 8	71 ± 4
K496A	$(1.1 \pm 0.1) \times 10^5$	$(8.7 \pm 0.9) \times 10^{-4}$	7 ± 1	67 ± 6	60 ± 4
H497A	$\mathbf{(1.8 \pm 0.2) \times 10^5}$	$\mathbf{(1.3 \pm 0.2) \times 10^{-3}}$	$\mathbf{7 \pm 2}$	$\mathbf{97 \pm 9}$	$\mathbf{104 \pm 7}$
K499A	$(1.5 \pm 0.2) \times 10^5$	$(1.2 \pm 0.2) \times 10^{-3}$	8 ± 2	42 ± 5	31 ± 3
K510A	$(2.1 \pm 0.3) \times 10^5$	$(1.7 \pm 0.3) \times 10^{-3}$	8 ± 2	28 ± 4	22 ± 3
K512A	$(1.6 \pm 0.2) \times 10^5$	$(1.1 \pm 1.2) \times 10^{-3}$	7 ± 2	15 ± 2	8 ± 2
K523A	$(1.9 \pm 0.2) \times 10^5$	$(1.3 \pm 0.1) \times 10^{-3}$	7 ± 2	97 ± 9	99 ± 6
K556A	$(1.2 \pm 0.1) \times 10^5$	$(9.0 \pm 1.3) \times 10^{-4}$	8 ± 1	12 ± 2	5 ± 1
K466A/R489A	$(1.0 \pm 0.2) \times 10^5$	$(1.0 \pm 0.1) \times 10^{-3}$	10 ± 2	25 ± 3	13 ± 1
R471A/R484A	$(1.1 \pm 0.2) \times 10^5$	$(8.8 \pm 0.6) \times 10^{-4}$	8 ± 1	10 ± 2	8 ± 2
S488A/R499A	$(9.6 \pm 0.9) \times 10^4$	$(8.6 \pm 0.7) \times 10^{-4}$	9 ± 1	35 ± 4	30 ± 2
R490A/H497A	$\mathbf{(1.3 \pm 0.1) \times 10^5}$	$\mathbf{(1.2 \pm 0.2) \times 10^{-3}}$	$\mathbf{9 \pm 2}$	$\mathbf{80 \pm 6}$	$\mathbf{76 \pm 5}$
K380A/K523A	$(8.7 \pm 0.9) \times 10^4$	$(1.6 \pm 0.2) \times 10^{-3}$	18 ± 3	49 ± 5	43 ± 3

[a] The A1/A3−C1−C2 fVIII heterodimer was immobilized on a sensor chip and tested for binding with A2 mutants and wt-A2 in a SPR-based assay, as described in Experimental Procedures. The corresponding kinetic constants were calculated using a one-site binding model. The activity of chimeric molecules of fVIIIa reconstituted from each A2 form and A1/A3−C1−C2 was tested in chromogenic and clotting assays (Experimental Procedures). The values are expressed as a percentage of the activity of fVIIIa reconstituted using wt-A2. A2 mutants with reduced affinity for LRP, which showed near-normal activity, are shown in bold. Data represent the means and SD obtained in three measurements for each assay.

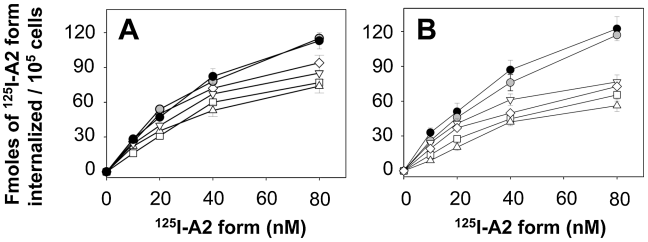

FIGURE 6: Internalization of selected A2 mutants by LRP-expressing cells. ^{125}I-labeled A2 forms were incubated at the indicated concentrations with monolayers of MEF cells for 4 h: (A) wt-A2 (●) and A2 single-point mutants L491A (gray circles), K466A (△), R484A (□), S488A (▽), and R489A (◇) and (B) wt-A2 (○, black) and A2 double-point mutants K380A/K512A (gray circles), K466A/R489A (□), R471A/R484A (△), S488A/K499A (▽), and R490A/H497A (◇). Internalized radioactivity was measured as described in Experimental Procedures. Each data point represents the mean and SD of duplicate determinations.

previous finding that the initial A2 binding to the cell surface is mediated by heparan sulfate proteoglycans (*30*). In contrast, RAP inhibited internalization of all A2 forms to a similar level constituting ~20% of that of wt-A2, A2 L491A, or A2 K380A/K523A. This confirms the role of LRP in the internalization process and reflects the existence of an additional, LRP-independent mechanism of A2 internalization (*20*, *30*). With this component considered, the decrease in the level of LRP-mediated internalization of A2 mutants is significant. In a parallel experiment with the same cell type genetically deficient in LRP (PEA 13), we found that the levels of surface binding and internalization of all A2 forms were the same (data not shown), additionally confirming the involvement of LRP in the experiments with MEF cells. Thus, the reduction in the affinity of the tested A2 single-point mutants for LRP correlated with their reduced level of internalization via this receptor in cell culture. For the double-point mutants, these effects were cumulative, further supporting the importance of the mutated residues for binding of A2 to LRP. On the basis of the collective data from experiments in a purified system and in cell culture, we conclude that residues K466, R471, R484, S488, R489, R490, H497, and K499 are critical in the formation of the binding epitope of A2 for LRP.

Clearance of A2 and Its Selected Mutants from the Circulation in Mice. The increase in the affinity of the A2 site for LRP upon activation of fVIII and the ability of isolated A2 to be internalized via LRP by cultured cells suggest its involvement in clearance of A2 as a product of dissociation of fVIIIa in vivo (*32*−*34*). This hypothesis was tested in mice in a manner similar to our previous study that established the role of LRP in the clearance of fVIII (*20*). We compared the clearance of ^{125}I-labeled pd-A2, injected in the circulation alone or with RAP, also using [^{125}I]fVIII as a control. In a parallel experiment, we tested the clearance of the [^{125}I]A2 double-point mutants R471A/R484A, which showed the greatest decrease in the affinity for LRP, and K380A/K523A with an unaffected affinity for LRP. The relative amounts of radioactivity in blood samples withdrawn within 1−180 min of injection were fitted to a double-exponential model previously used in studies of fVIII clearance (*20*, *23*). We found that the half-life of A2 (16 ± 4 min) was ~4.5 times shorter than the half-life of injected fVIII (72 ± 14 min) (Figure 7), correlating with an affinity of A2 for LRP higher than that of fVIII (K_D = 80−116 nM) (*20*, *26*). Approximately 80% of the injected radioactivity

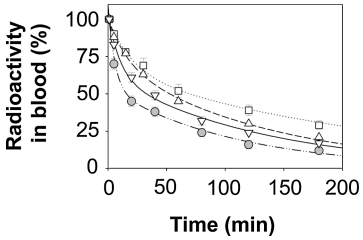

FIGURE 7: Clearance of A2 and A2 mutant R471A/R484A from the circulation of mice. [^{125}I]r-A2, alone at 100 nM (grey circles, dotted−dotted−dashed line) or with 200 μM RAP (△, dashed line), [^{125}I]A2 R471A/R484A at 100 nM (▽, solid line), or [^{125}I]fVIII at 100 nM (□, dotted line) in 100 μL of HBS-Ca buffer was injected into the tail vein of BALB/c mice ($n = 4$). Blood samples were withdrawn at indicated time points (1−180 min) and measured for radioactivity normalized to sample volumes. The values are expressed as a percentage of the initial sample count (at the 1 min point). The data represent the means and the SD, and the lines represent fits to a double-exponential decay model.

accumulated in the liver where LRP (and LDLR) is expressed abundantly. Noteworthy is the fact that the half-life of injected fVIII was similar to that of fVIII from the fVIII−vWf complex (65 ± 12 min) in the same strain of mice (*20*, *26*), likely due to a rapid formation of the complex with intrinsic vWf as mouse vWf and human vWf have similar affinities for human fVIII (*64*). The co-injection of RAP resulted in an ~3.5-fold prolongation of the A2 half-life (56 ± 9 min), suggesting the involvement of a receptor(s) from the LDLR family, likely LRP (and LDLR), in the clearance of A2. In turn, the half-life of A2 mutant R471A/R484A (30 ± 7 min) was ~1.9 times longer than that of the control A2 mutant K380A/K523A (18 ± 4 min), the half-life of which was very similar to that of wt-A2. Thus, in vivo experiments confirmed the importance of the mutated A2 residues for the interaction with LRP and suggested a function for LRP in removing A2 from the circulation upon dissociation of fVIIIa.

DISCUSSION

In this study, we determined the critical amino acid residues of the fVIII A2 domain, which are responsible for its binding to LRP. Isolated A2 was subjected to alanine-scanning mutagenesis, which represents a commonly used technique for studying binding sites of proteins (*65*, *66*). A series of single-point mutations was introduced within and in the proximity of the A2 region of residues 484−509, shown previously to be involved in binding to LRP (*20*, *31*). For a number of A2 mutants, their decreased affinity for LRP correlated with a reduced level of internalization via this receptor by cultured cells. Importantly, combination of these mutations in pairs produced cumulative effects on the binding of double-point A2 mutants to LRP and their LRP-mediated internalization in cell culture. Most mutants with reduced affinity for LRP retained cofactor activity in reconstituted fVIIIa, further confirming that these mutations specifically targeted the binding epitope for LRP. On the basis of the collected experimental evidence, A2 residues K466, R471, R484, S488, R489, R490, H497, and K499 were identified as being major determinants of the A2 binding site for LRP (Figure 8).

The comparison of amino acid sequences among human, porcine, canine, and murine fVIII molecules (http://europium.csc.mrc.ac.uk) reveals that five of the identified residues are conservative, whereas less homology is observed for the R484, S488, and R489 positions. Among the identified residues, positions K466 and R471 do not belong to the region of residues 484−509 but are spatially adjacent to it on the A2 surface, thus extending the previously proposed area of the A2 binding site for LRP.

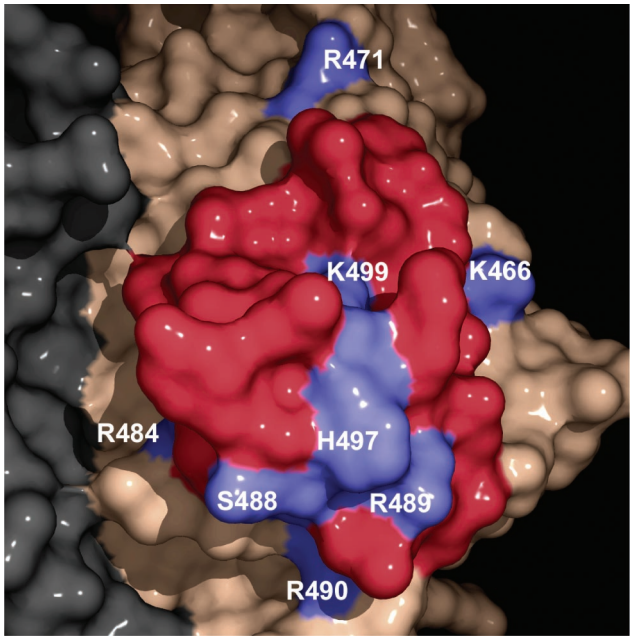

FIGURE 8: Binding epitope of the fVIII A2 domain for LRP. The fragment of the atomic model of fVIII was generated as described in the legend of Figure 1. A2 residues, which mostly contribute to interaction with LRP, are colored blue. The region of residues 484−509 is colored red. Other residues of A2 and the residues of the A1 domain are colored beige and gray, respectively.

The observed reduction in affinities for LRP of the above eight A2 single-point mutants was generally moderate. This can be explained by our most recent finding that within LRP clusters II and IV, the sites for A2 are multiple. Each elementary site is formed by two adjacent CRs interacting with A2 likely in a nonidentical way, which is evident from different effects of mutations on the A2 affinity for short fragments overlapping clusters II and IV (*67*). Therefore, it is likely that each A2 mutation affects the binding to certain but not all elementary sites in LRP, and the determined affinities correspond to the persisting interactions.

Additional evidence for the critical role of the identified A2 residues in the formation of the binding epitope for LRP comes from previous reports that fVIII interacts with two other members of the LDLR family, VLDLR and megalin (*68*, *69*), and our recent finding that A2 is also able to bind to these receptors with high affinity ($K_D = 15-20$ nM). We demonstrated that most mutations, important for binding of A2 to LRP, also led to a reduction in the affinity of A2 for VLDLR and megalin (*70*). Thus, the identified A2 residues seem to form a universal binding epitope for LRP, VLDLR, and megalin. Notably, the decrease in affinity of A2 mutants was more pronounced for VLDLR. This is consistent with its relatively simple structure (*71*) that is able to provide significantly lower numbers of potential sites for A2 than LRP, as can be predicted from the data of Andersen for RAP−LRP interaction (*72*, *73*).

Important details of interactions of LDLR family receptors with their ligands were revealed in a study in which a pair of adjacent CRs of LDLR was tested for binding with its β-propeller domain, which displaces bound ligands at low pH in endosomes and thus can be used as a model of any ligand (*53*). On the receptor side, this binding involves a specific cluster of negatively charged residues, stabilized by Ca^{2+} ion and presented on each CR. Each cluster interacts with a positively charged residue on the ligand side. In the β-propeller domain, the distance between the α-carbons of two lysines, involved in the binding, is 12.4 Å. Noteworthy is the fact that this distance is comparable with that between A2 residues, which had the strongest effect on the binding to LRP (K466, R471, and R489, 12−16 Å). In addition, variable-length flexible connectors between adjacent CRs (*74*, *75*) could provide a flexibility in the ligands' recognition, in particular, in recognition of A2 by multiple CR pairs of LRP.

In this work, we also demonstrated the existence of a mechanism for removal of A2 from the circulation via LRP (and possibly other members of the LDLR family) that is consistent with a higher affinity of A2 for LRP in comparison with that for fVIII. Notably, the other product of fVIIIa dissociation, the A1/A3−C1−C2 heterodimer, also has a higher affinity for LRP than fVIII, can be internalized via LRP in cell culture (*67*), and can be cleared via LRP from mice circulation (A. Sarafanov, unpublished data). These results indicate that LRP may be involved in clearance of both products of dissociated fVIIIa, though the bulk of the A1/A3−C1−C2 moiety is likely to remain associated with platelets at the sites of clot formation. Considering the fact that fV, fVII, and fIX are able to interact with LRP only in activated forms (*10*−*12*), it is possible that LRP plays a role in coagulation control via removal of certain activated factors.

Besides interaction with LRP, the region of residues 484−509 of fVIII is also involved in other physiological interactions. It represents one of the major epitopes for inhibitory antibodies which often develop in hemophilia A patients in response to infusions of fVIII, with the main immunogenic residues being R484, Y487, S488, R489, P492, V495, P501, and I508 (*56*, *76*, *77*). Mutation of these residues into alanine might decrease the immunogenicity of fVIII (*78*). The region of residues 484−509 also contributes to fVIIIa cofactor activity for fIXa (*60*). In this respect, it is worthwhile to compare relative activities of fVIIIa reconstituted with our generated A2 mutants with reported activities of some fVIII mutants. The decreased activities of A2 mutants K466A, R471A, and K510A correlate with the hemophilia A phenotype of natural mutations K466T, R471G, and K510E in fVIII (http://europium.csc.mrc.ac.uk). The near-normal activities of A2 mutants R484A, S488A, R489A, R490A, and K493A correlate with activities of artificial fVIII mutants with the same substitutions (*60*, *77*, *78*).

Identification of mutations which do not affect the activity of fVIII but weaken its interaction with catabolic receptors is related to the idea of prolonging fVIII lifetime in the circulation for more efficient treatment of hemophilia A. In this respect, mutagenesis of the isolated A2 domain is the first step in identifying the critical residues that govern interaction of full-length fVIII with LRP. Further mutagenic experiments on full-length fVIII will be required to verify whether mutations of A2 residues, selected in this study, will have similar effects on fVIII−LRP interaction and the fVIII lifetime in the circulation. Mutations R484A, S488A, R489A, R490A, and H497A, which resulted in reduced affinity of A2 for LRP while retaining the cofactor activity, may be good candidates for introduction into full-length fVIII. Studies of LRP-mediated catabolism of these fVIII mutants from their complexes with vWf will allow the revelation of more specifically the role of the LRP-binding site within A2 in this process. Identification of the LRP-binding epitope within A2 also raises a question of whether the binding sites of the A2 domain (and within the fVIII LCh) for LRP and LDLR are similarly organized. It could be expected that prolongation of the fVIII lifetime will result from mutating specific residues important for interaction of fVIII with both LRP and LDLR.

REFERENCES

1. Saenko, E. L., Ananyeva, N. M., Tuddenham, E. G., and Kemball-Cook, G. (2002) Factor VIII: Novel insights into form and function, *Br. J. Haematol. 119*, 323−331.
2. Fay, P. (1999) Regulation of factor VIIIa in the intrinsic factor Xase, *Thromb. Haemostasis 82*, 193−200.
3. Vehar, G. A., Keyt, B., Eaton, D., Rodriguez, H., O'Brien, D. P., Rotblat, F., Oppermann, H., Keck, R., Wood, W. I., and Harkins, R. N. (1984) Structure of human factor VIII, *Nature 312*, 337−342.
4. Kaufman, R. J., Wasley, L. C., and Dorner, A. J. (1988) Synthesis, processing, and secretion of recombinant human factor VIII expressed in mammalian cells, *J. Biol. Chem. 263*, 6352−6362.
5. Lollar, P., Hill-Eubanks, D. C., and Parker, C. G. (1988) Association of the factor VIII light chain with von Willebrand factor, *J. Biol. Chem. 263*, 10451−10455.
6. Fay, P. J., Haidaris, P. J., and Smudzin, T. M. (1991) Human factor VIIIa subunit structure. Reconstruction of factor VIIIa from the isolated A1/A3-C1-C2 dimer and A2 subunit, *J. Biol. Chem. 266*, 8957−8962.
7. Saenko, E. L., Shima, M., and Sarafanov, A. G. (1999) Role of activation of the coagulation factor VIII in interaction with vWf, phospholipid, and functioning within the factor Xase complex, *Trends Cardiovasc. Med. 9*, 185−192.
8. Herz, J., Hamann, U., Rogne, S., Myklebost, O., Gausepohl, H., and Stanley, K. K. (1988) Surface location and high affinity for calcium of a 500-kd liver membrane protein closely related to the LDL-receptor suggest a physiological role as lipoprotein receptor, *EMBO J. 7*, 4119−4127.
9. Strickland, D. K., and Ranganathan, S. (2003) Diverse role of LDL receptor-related protein in the clearance of proteases and in signaling, *J. Thromb. Haemostasis 1*, 1663−1670.
10. Bos, M. H. A., Bovenschen, N., Boertjes, R. C., Van Der Zwaan, C., Van Rhenen, K., Hilkes, Y. H. A., Meijer, A. B., and Mertens, K. (2003) Exposure of a binding site for the low-density lipoprotein receptor-related protein (LRP) upon activation of factor V, *J. Thromb. Haemostasis 1* (Suppl. 1), Abstract OC096.
11. Iakhiaev, A., Pendurthi, U. R., Voigt, J., Ezban, M., and Vijaya Mohan, R. L. (1999) Catabolism of factor VIIa bound to tissue factor in fibroblasts in the presence and absence of tissue factor pathway inhibitor, *J. Biol. Chem. 274*, 36995−37003.
12. Neels, J. G., van Den Berg, B. M., Mertens, K., ter Maat, H., Pannekoek, H., van Zonneveld, A. J., and Lenting, P. J. (2000) Activation of factor IX zymogen results in exposure of a binding site for low-density lipoprotein receptor-related protein, *Blood 96*, 3459−3465.
13. Warshawsky, I., Broze, G. J., Jr., and Schwartz, A. L. (1994) The low-density lipoprotein receptor-related protein mediates the cellular degradation of tissue factor pathway inhibitor, *Proc. Natl. Acad. Sci. U.S.A. 91*, 6664−6668.
14. Neels, J. G., Horn, I. R., van Den Berg, B. M., Pannekoek, H., and van Zonneveld, A. J. (1998) Ligand−receptor interactions of the low-density lipoprotein receptor-related protein, a multi-ligand endocytic receptor, *Fibrinolysis Proteolysis 12*, 219−240.
15. Esser, V., Limbird, L. E., Brown, M. S., Goldstein, J. L., and Russell, D. W. (1988) Mutational analysis of the ligand binding domain of the low-density lipoprotein receptor, *J. Biol. Chem. 263*, 13282−13290.

16. Russell, D. W., Brown, M. S., and Goldstein, J. L. (1989) Different combinations of cysteine-rich repeats mediate binding of low-density lipoprotein receptor to two different proteins, *J. Biol. Chem. 264*, 21682−21688.
17. Neels, J. G., van Den Berg, B. M., Lookene, A., Olivecrona, G., Pannekoek, H., and van Zonneveld, A. J. (1999) The second and fourth cluster of class A cysteine-rich repeats of the low-density lipoprotein receptor-related protein share ligand-binding properties, *J. Biol. Chem. 274*, 31305−31311.
18. Bu, G., and Rennke, S. (1996) Receptor-associated protein is a folding chaperone for low-density lipoprotein receptor-related protein, *J. Biol. Chem. 271*, 22218−22224.
19. Obermoeller, L. M., Warshawsky, I., Wardell, M. R., and Bu, G. (1997) Differential functions of triplicated repeats suggest two independent roles for the receptor-associated protein as a molecular chaperone, *J. Biol. Chem. 272*, 10761−10768.
20. Saenko, E. L., Yakhyaev, A. V., Mikhailenko, I., Strickland, D. K., and Sarafanov, A. G. (1999) Role of the low-density lipoprotein-related protein receptor in mediation of factor VIII catabolism, *J. Biol. Chem. 274*, 37685−37692.
21. Turecek, P. L., Schwarz, H. P., and Binder, B. R. (2000) In vivo inhibition of low-density lipoprotein receptor-related protein improves survival of factor VIII in the absence of von Willebrand factor, *Blood 95*, 3637−3638.
22. Schwarz, H. P., Lenting, P. J., Binder, B., Mihaly, J., Denis, C., Dorner, F., and Turecek, P. L. (2000) Involvement of low-density lipoprotein receptor-related protein (LRP) in the clearance of factor VIII in von Willebrand factor-deficient mice, *Blood 95*, 1703−1708.
23. Bovenschen, N., Herz, J., Grimbergen, J. M., Lenting, P. J., Havekes, L. M., Mertens, K., and van Vlijmen, B. J. (2003) Elevated plasma factor VIII in a mouse model of low-density lipoprotein receptor-related protein deficiency, *Blood 101*, 3933−3939.
24. Bovenschen, N., Mertens, K., Hu, L., Havekes, L. M., and van Vlijmen, B. J. (2005) LDL receptor cooperates with LDL receptor-related protein in regulating plasma levels of coagulation factor VIII in vivo, *Blood 106*, 906−912.
25. Bovenschen, N., Boertjes, R. C., van Stempvoort, G., Voorberg, J., Lenting, P. J., Meijer, A. B., and Mertens, K. (2003) Low-density lipoprotein receptor-related protein and factor IXa share structural requirements for binding to the A3 domain of coagulation factor VIII, *J. Biol. Chem. 278*, 9370−9377.
26. Lenting, P. J., Neels, J. G., van Den Berg, B. M., Clijsters, P. P., Meijerman, D. W., Pannekoek, H., van Mourik, J. A., Mertens, K., and van Zonneveld, A. J. (1999) The light chain of factor VIII comprises a binding site for low-density lipoprotein receptor-related protein, *J. Biol. Chem. 274*, 23734−23739.
27. Lenting, P. J., Donath, M. J., van Mourik, J. A., and Mertens, K. (1994) Identification of a binding site for blood coagulation factor IXa on the light chain of human factor VIII, *J. Biol. Chem. 269*, 7150−7155.
28. Saenko, E. L., and Scandella, D. (1997) The acidic region of the factor VIII light chain and the C2 domain together form the high affinity binding site for von Willebrand factor, *J. Biol. Chem. 272*, 18007−18014.
29. Lethagen, S., Berntorp, E., and Nilsson, I. M. (1992) Pharmacokinetics and hemostatic effect of different factor VIII/von Willebrand factor concentrates in von Willebrand's disease type III, *Ann. Hematol. 65*, 253−259.
30. Sarafanov, A. G., Ananyeva, N. M., Shima, M., and Saenko, E. L. (2001) Cell surface heparan sulfate proteoglycans participate in factor VIII catabolism mediated by low-density lipoprotein receptor-related protein, *J. Biol. Chem. 276*, 11970−11979.
31. Bovenschen, N., Van Stempvoort, G., Voorberg, J., Mertens, K., and Meijer, A. (2003) Cleavage of factor VIII heavy chain by thrombin increases the affinity for low-density lipoprotein receptor-related protein (LRP), *J. Thromb. Haemostasis 1* (Suppl. 1), Abstract OC095.
32. Fay, P. J., and Smudzin, T. M. (1992) Characterization of the interaction between the A2 subunit and A1/A3-C1-C2 dimer in human factor VIIIa, *J. Biol. Chem. 267*, 13246−13250.
33. Fay, P. J., Beattie, T. L., Regan, L. M., O'Brien, L. M., and Kaufman, R. J. (1996) Model for the factor VIIIa-dependent decay of the intrinsic factor Xase. Role of subunit dissociation and factor IXa-catalyzed proteolysis, *J. Biol. Chem. 271*, 6027−6032.
34. Brinkman, H. J., Koster, P., Mertens, K., and van Mourik, J. A. (1997) Dissimilar interaction of factor VIII with endothelial cells and lipid vesicles during factor X activation, *Biochem. J. 323* (Part 3), 735−740.
35. Stoilova-McPhie, S., Villoutreix, B. O., Mertens, K., Kemball-Cook, G., and Holzenburg, A. (2002) 3-Dimensional structure of membrane-bound coagulation factor VIII: Modeling of the factor VIII heterodimer within a 3-dimensional density map derived by electron crystallography, *Blood 99*, 1215−1223.
36. Saenko, E. L., Shima, M., Gilbert, G. E., and Scandella, D. (1996) Slowed release of thrombin-cleaved factor VIII from von Willebrand factor by a monoclonal and a human antibody is a novel mechanism for factor VIII inhibition, *J. Biol. Chem. 271*, 27424−27431.
37. Lapan, K. A., and Fay, P. J. (1997) Localization of a factor X interactive site in the A1 subunit of factor VIIIa, *J. Biol. Chem. 272*, 2082−2088.
38. Lollar, P., Fay, P. J., and Fass, D. (1999) Factor VIII and Factor VIIIa, *Methods Enzymol. 222*, 128−143.
39. Ashcom, J. D., Tiller, S. E., Dickerson, K., Cravens, J. L., Argraves, W. S., and Strickland, D. K. (1990) The human α2-macroglobulin receptor: Identification of a 420-kD cell surface glycoprotein specific for the activated conformation of α2-macroglobulin, *J. Cell Biol. 110*, 1041−1048.
40. Williams, S. E., Ashcom, J. D., Argraves, W. S., and Strickland, D. K. (1992) A novel mechanism for controlling the activity of α2-macroglobulin receptor/low-density lipoprotein receptor-related protein. Multiple regulatory sites for 39-kDa receptor-associated protein, *J. Biol. Chem. 267*, 9035−9040.
41. Saenko, E. L., Shima, M., Rajalakshmi, K. J., and Scandella, D. (1994) A role for the C2 domain of factor VIII in binding to von Willebrand factor, *J. Biol. Chem. 269*, 11601−11605.
42. Barenholz, Y., Gibbes, D., Litman, B. J., Goll, J., Thompson, T. E., and Carlson, R. D. (1977) A simple method for the preparation of homogeneous phospholipid vesicles, *Biochemistry 16*, 2806−2810.
43. Katagiri, Y., and Ingham, K. C. (2002) Enhanced production of green fluorescent fusion proteins in a baculovirus expression system by addition of secretion signal, *BioTechniques 33*, 24−26.
44. Sarafanov, A., and Saenko, E. (2004) High-throughput optimization of protein expression in the baculovirus system based on determination of relative expression efficiency of viral stocks, *Anal. Biochem. 328*, 98−100.
45. Mertens, K., van Wijngaarden, A., and Bertina, R. M. (1985) The role of factor VIII in the activation of human blood coagulation factor X by activated factor IX, *Thromb. Haemostasis 54*, 654−660.
46. Rosen, S. (1984) Assay of factor VIII:C with a chromogenic substrate, *Scand. J. Haematol. Suppl. 40*, 139−145.
47. Casillas, G., Simonetti, C., and Pavlosky, A. (1971) Artificial substrate for the assay of factors V and VIII, *Coagulation 4*, 107−111.
48. Horn, I. R., van Den Berg, B. M., van der Meijden, P. Z., Pannekoek, H., and van Zonneveld, A. J. (1997) Molecular analysis of ligand binding to the second cluster of complement-type repeats of the low-density lipoprotein receptor-related protein. Evidence for an allosteric component in receptor-associated protein-mediated inhibition of ligand binding, *J. Biol. Chem. 272*, 13608−13613.
49. Persson, E., Ezban, M., and Shymko, R. M. (1995) Kinetics of the interaction between the human factor VIIIa subunits: Effects of pH, ionic strength, Ca^{2+} concentration, heparin, and activated protein C-catalyzed proteolysis, *Biochemistry 34*, 12775−12781.
50. Willnow, T. E., and Herz, J. (1994) Genetic deficiency in low-density lipoprotein receptor-related protein confers cellular resistance to *Pseudomonas* exotoxin A. Evidence that this protein is required for uptake and degradation of multiple ligands, *J. Cell Sci. 107* (Part 3), 719−726.
51. Chappell, D. A., Fry, G. L., Waknitz, M. A., Iverius, P. H., Williams, S. E., and Strickland, D. K. (1992) The low-density lipoprotein receptor-related protein/α2-macroglobulin receptor binds and mediates catabolism of bovine milk lipoprotein lipase, *J. Biol. Chem. 267*, 25764−25767.
52. Kounnas, M. Z., Chappell, D. A., Wong, H., Argraves, W. S., and Strickland, D. K. (1995) The cellular internalization and degradation of hepatic lipase is mediated by low-density lipoprotein receptor-related protein and requires cell surface proteoglycans, *J. Biol. Chem. 270*, 9307−9312.
53. Rudenko, G., Henry, L., Henderson, K., Ichtchenko, K., Brown, M. S., Goldstein, J. L., and Deisenhofer, J. (2002) Structure of

the LDL receptor extracellular domain at endosomal pH, *Science 298*, 2353−2358.
54. Melman, L., Cao, Z. F., Rennke, S., Marzolo, M. P., Wardell, M. R., and Bu, G. (2001) High affinity binding of receptor-associated protein to heparin and low-density lipoprotein receptor-related protein requires similar basic amino acid sequence motifs, *J. Biol. Chem. 276*, 29338−29346.
55. Lalazar, A., Weisgraber, K. H., Rall, S. C., Jr., Giladi, H., Innerarity, T. L., Levanon, A. Z., Boyles, J. K., Amit, B., Gorecki, M., and Mahley, R. W. (1988) Site-specific mutagenesis of human apolipoprotein E. Receptor binding activity of variants with single amino acid substitutions, *J. Biol. Chem. 263*, 3542−3545.
56. Healey, J. F., Lubin, I. M., Nakai, H., Saenko, E. L., Hoyer, L. W., Scandella, D., and Lollar, P. (1995) Residues 484−508 contain a major determinant of the inhibitory epitope in the A2 domain of human factor VIII, *J. Biol. Chem. 270*, 14505−14509.
57. Fulcher, C. A., Roberts, J. R., Holland, L. Z., and Zimmerman, T. S. (1985) Human factor VIII procoagulant protein. Monoclonal antibodies define precursor-product relationships and functional epitopes, *J. Clin. Invest. 76*, 117−124.
58. Fay, P. J., Smudzin, T. M., and Walker, F. J. (1991) Activated protein C-catalyzed inactivation of human factor VIII and factor VIIIa. Identification of cleavage sites and correlation of proteolysis with cofactor activity, *J. Biol. Chem. 266*, 20139−20145.
59. Koszelak, M. E., Huggins, C. F., and Fay, P. J. (2000) Sites in the A2 subunit involved in the interfactor VIIIa interaction, *J. Biol. Chem. 275*, 27137−27144.
60. Jenkins, P. V., Dill, J. L., Zhou, Q., and Fay, P. J. (2004) Clustered basic residues within segment 484−510 of the factor VIIIa A2 subunit contribute to the catalytic efficiency for factor Xa generation, *J. Thromb. Haemostasis 2*, 452−458.
61. Jenkins, P. V., Freas, J., Schmidt, K. M., Zhou, Q., and Fay, P. J. (2002) Mutations associated with hemophilia A in the 558−565 loop of the factor VIIIa A2 subunit alter the catalytic activity of the factor Xase complex, *Blood 100*, 501−508.
62. Bajaj, S. P., Schmidt, A. E., Mathur, A., Padmanabhan, K., Zhong, D., Mastri, M., and Fay, P. J. (2001) Factor IXa:factor VIIIa interaction. Helix 330−338 of factor ixa interacts with residues 558−565 and spatially adjacent regions of the A2 subunit of factor VIIIa, *J. Biol. Chem. 276*, 16302−16309.
63. Fay, P. J., and Koshibu, K. (1998) The A2 subunit of factor VIIIa modulates the active site of factor IXa, *J. Biol. Chem. 273*, 19049−19054.
64. Kawasaki, T., Kaida, T., Arnout, J., Vermylen, J., and Hoylaerts, M. F. (1999) A new animal model of thrombophilia confirms that high plasma factor VIII levels are thrombogenic, *Thromb. Haemostasis 81*, 306−311.
65. Cunningham, B. C., and Wells, J. A. (1989) High-resolution epitope mapping of hGH-receptor interactions by alanine-scanning mutagenesis, *Science 244*, 1081−1085.
66. Jin, L., and Wells, J. A. (1994) Dissecting the energetics of an antibody−antigen interface by alanine shaving and molecular grafting, *Protein Sci. 3*, 2351−2357.
67. Sarafanov, A., Makogonenko, E., Andersen, O., Khrenov, A., Mikhailenko, A., Ananyeva, A., Strickland, D., and Saenko, E. (2005) Fragments of Activated Coagulation Factor VIII Bind to Multiple Sites within Low-Density Lipoprotein Receptor-Related Protein, *Blood 106* (11), 298a (Abstract 1019).
68. Mertens, K., Bovenschen, N., Voorberg, J., and Meijer, A. (2003) The Endocytic Receptors Megalin and Low-Density Lipoprotein Receptor-Related Protein Share Binding to Coagulation Factor VIII, *Blood 102* (11), 89a (Abstract 302).
69. Kouiavskaia, D., Ruiz, J., Strickland, D., and Saenko, E. (2003) Very Low-Density Lipoprotein Receptor Interacts with Coagulation Factor VIII, *Blood 102* (11), 88a (Abstract 301).
70. Makogonenko, E., Sarafanov, A., Pechik, I., Andresen, O., Ananyeva, N., Radtke, K.-P., Strickland, D., and Saenko, E. (2005) The A2 Domain of Coagulation Factor VIII Shares Residues Critical for Interaction with three members of LDL Receptor Superfamily: LRP, VLDL and Megalin receptors, *J. Thromb. Haemostasis 3* (Suppl. 1), Abstract P0646.
71. Verdaguer, N., Fita, I., Reithmayer, M., Moser, R., and Blaas, D. (2004) X-ray structure of a minor group human rhinovirus bound to a fragment of its cellular receptor protein, *Nat. Struct. Mol. Biol. 11*, 429−434.
72. Andersen, O. M., Christensen, L. L., Christensen, P. A., Sorensen, E. S., Jacobsen, C., Moestrup, S. K., Etzerodt, M., and Thogersen, H. C. (2000) Identification of the minimal functional unit in the low-density lipoprotein receptor-related protein for binding the receptor- associated protein (RAP). A conserved acidic residue in the complement-type repeats is important for recognition of RAP, *J. Biol. Chem. 275*, 21017−21024.
73. Andersen, O. M., Petersen, H. H., Jacobsen, C., Moestrup, S. K., Etzerodt, M., Andreasen, P. A., and Thogersen, H. C. (2001) Analysis of a two-domain binding site for the urokinase-type plasminogen activator-plasminogen activator inhibitor-1 complex in low-density-lipoprotein-receptor-related protein, *Biochem. J. 357*, 289−296.
74. Beglova, N., North, C. L., and Blacklow, S. C. (2001) Backbone dynamics of a module pair from the ligand-binding domain of the LDL receptor, *Biochemistry 40*, 2808−2815.
75. Kurniawan, N. D., Atkins, A. R., Bieri, S., Brown, C. J., Brereton, I. M., Kroon, P. A., and Smith, R. (2000) NMR structure of a concatemer of the first and second ligand-binding modules of the human low-density lipoprotein receptor, *Protein Sci. 9*, 1282−1293.
76. Ananyeva, N. M., Lacroix-Desmazes, S., Hauser, C. A., Shima, M., Ovanesov, M. V., Khrenov, A. V., and Saenko, E. L. (2004) Inhibitors in hemophilia A: Mechanisms of inhibition, management and perspectives, *Blood Coagulation Fibrinolysis 15*, 109−124.
77. Lubin, I. M., Healey, J. F., Barrow, R. T., Scandella, D., and Lollar, P. (1997) Analysis of the human factor VIII A2 inhibitor epitope by alanine scanning mutagenesis, *J. Biol. Chem. 272*, 30191−30195.
78. Parker, E. T., Healey, J. F., Barrow, R. T., Craddock, H. N., and Lollar, P. (2004) Reduction of the inhibitory antibody response to human factor VIII in hemophilia A mice by mutagenesis of the A2 domain B-cell epitope, *Blood 104*, 704−710.

BI0520380